



Contents lists available at ScienceDirect

# Engineering Failure Analysis

journal homepage: [www.elsevier.com/locate/engfailanal](http://www.elsevier.com/locate/engfailanal)

## Integrity assessment and determination of residual fatigue life of vital parts of bucket-wheel excavator operating under dynamic loads



Dušan Arsić<sup>a,\*</sup>, Nebojša Gnjatović<sup>b</sup>, Simon Sedmak<sup>c</sup>, Aleksandra Arsić<sup>b</sup>,  
Milan Uhrčik<sup>d</sup>

<sup>a</sup> Faculty of Engineering, University of Kragujevac, Sestre Janjić 6 St., 34000 Kragujevac, Serbia

<sup>b</sup> Faculty of Mechanical Engineering, University of Belgrade, Kraljice Marije 16 St., 11000 Belgrade, Serbia

<sup>c</sup> Innovation Centre of the Faculty of Mechanical Engineering, University of Belgrade, Kraljice Marije 16 St., 11000 Belgrade, Serbia

<sup>d</sup> Faculty of Mechanical Engineering, University of Žilina, Univerzitná 8215/1 St., 010 26 Žilina, Slovakia

### ARTICLE INFO

#### Keywords:

Bucket-wheel excavator  
Oscillations  
Stress condition  
Fatigue crack  
Service life

### ABSTRACT

In this paper are presented results of tests and analyses of complex dynamic loads carried out on the bucket-wheel excavator SchRs 650/5 × 24 Krupp, as well as assessment of service life of vital welded structures of a bucket-wheel excavator boom subjected to cyclic loading with a variable amplitude through the use of experimental tests carried out in order to determine operational strength and growth of a fatigue crack for one structural part. Bucket-wheel excavator was built by “Thyssen Krupp” company, Germany. Outer loads, or in other words digging forces for the overburden and coal have been calculated on the basis of measured values of actual current intensity of the bucket-wheel drive and recorded output values of changeable loads. Correlations between the power of the bucket-wheel drive system and adequate hourly production, depending on the overall digging resistance which affects the stress condition of the bucket-wheel, were also determined. Results of the theoretical and experimental analysis of natural and forced oscillations of the support structure for various exploitation conditions are presented in first part of the paper. Deformations  $\varepsilon_i$  determined by tensometric measurements on the rotating shaft of the bucket-wheel were converted into tangential stresses through the introduction of the modulus of elasticity and Poisson's ratio, which, along with the polar moment of inertia of the cross-section, define the moment of rotation on the bucket-wheel shaft. Through the use of the load - strength comparison method (maximization of the ratio of load and strength indicators) the application factor of the gear with the largest number of turns  $K_A$  has been determined.

In the second part of the paper methodological approach for the assessment of service life of vital welded structures of a bucket-wheel excavator boom was presented. Assessment was done in order to determine operational strength and growth of a fatigue crack, through the use of experimental tests. Realized researches and results presented in this paper offer great possibilities for the analyses of behaviour of vital welded structures of the bucket-wheel boom. By the application of the measurement device with 8 channels for registration and processing of electric signals HBM Spider 8 and measurement tapes HBM 6/350 × XY31 deformations were measured at vital welded structures of the boom in the area of the bucket-wheel. The objective of the test is

\* Corresponding author.

E-mail address: [dusan.arsic@fink.rs](mailto:dusan.arsic@fink.rs) (D. Arsić).

<https://doi.org/10.1016/j.engfailanal.2019.06.072>

Received 10 January 2019; Received in revised form 21 June 2019; Accepted 22 June 2019

Available online 29 June 2019

1350-6307/ © 2019 Elsevier Ltd. All rights reserved.

to determine if there is a possibility of occurrence of plastic deformations or initial cracks due to fatigue at vital welded structures and to obtain data which define crack growth.

## 1. Introduction

Bucket-wheel excavators in exploitation are subjected to stresses which occur during the production of components and equipment assembling (residual stresses), during the process of performing functional tasks (stationary and dynamic loads), as well as during the disturbed process of exploitation (non-stationary dynamic loads). Therefore, loads of important components and structural elements of bucket-wheel excavators cannot be expressed in the form of a simple mathematical function, and accordingly cannot be fully presented by a model in which variables or parameters change uniformly in exploitation conditions, because such a model predicts a string of approximations, which depend on real conditions of production and exploitation.

Tests of bucket-wheel excavator structures in operating conditions enable the full evaluation of their condition and acquisition of data necessary for quality comparison and evaluation of machines and structures, for the evaluation of the spatial operation of singular components and elements regarding the load carrying capacity, as well as the determination of the possibility of mutual operation of drive units and structures [1–7].

SchRs 650/5 × 24 bucket-wheel excavator operates at largest excavation site in Serbia's autonomus province Kosovo and Metohija called “Dobro Selo” in Obilić. Basic technical and technological characteristics of the excavator are presented in Fig. 1 [8,9].

## 2. Dynamic loads at the bucket-wheel excavator during service

Most components and elements of vital structures of bucket-wheel excavators are subjected to complex dynamic loads, which depend on conditions of exploitation (resistance to digging and own oscillations) in the stationary and non-stationary operational regimes of bucket-wheel excavator drive systems during service [10,11]. Oscillations of excavator's elements can also cause certain stability problems [12,13].

### 2.1. Digging resistance

Determination of the outer load on the bucket-wheel which occurs due to digging resistance is essential during the design process and exploitation. There is a large number of parameters which define the resistances during the digging process, and they are divided into 3 groups: rock mass parameters, geometric digging parameters and constructive kinetic properties of the excavator.

#### 2.1.1. Theoretical analysis

The bucket-wheel with buckets has to overcome resistances which occur due to cutting, lifting of the dug material, filling of buckets and friction between the material and the ground, as well as between the material and the buckets, which all depend on cutting parameters and characteristics of the operating environment. In practice it is necessary to determine overall resistances in order to provide necessary basis for the selection and dimensioning of the bucket-wheel excavator (Fig. 2).

Basic component of the digging resistance is the tangential component  $F_t$  [kN], defined as the product of the specific linear digging resistance per knife length [kN/m] and the sum of average lengths of cutting edges of knives in operation  $L_{sr}$  [m], or a

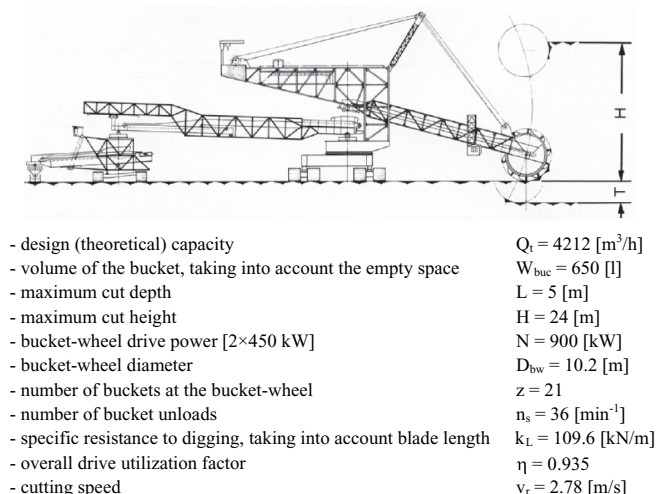


Fig. 1. Schematic appearance and technical data of the bucket-wheel excavator SchRs 650/5 × 24.

Nomenclature			
$Q_t$	Design (theoretical) capacity	$f$	Frequencies of natural oscillations for the approximate model of the bucket-wheel boom
$W_{buc}$	Volume of the bucket, taking into account the empty space	$Q_e$	Hourly production of the excavator
$L$	Maximum cut depth	$\sigma$	Normal stress
$H$	Maximum cut height	$\sigma_1$	Calculated normal stress
$N$	Bucket-wheel drive power [ $2 \times 450$ kW]	$\tau$	Tangential stress
$D_{bw}$	Bucket-wheel diameter	$\varepsilon$	Normal deformation
$z$	Number of buckets at the bucket-wheel	$W_p$	Polar moment of inertia of the bucket-wheel drive shaft cross-section
$n_s$	Number of bucket unloads	$T_i$	Torsional moments of rotation
$k_L$	Specific resistance to digging, taking into account blade length	$K_A$	Application factor for the gear with the largest number of revolutions in gearbox for excavator moving
$\eta$	Overall drive utilization factor	$T_{eq}$	Equivalent torque
$v_r$	Cutting speed	$T_n$	Nominal torque
$F_t$	Tangential component of the digging resistance	$da/dN$	Fatigue crack growth rate
$L_{sr}$	Sum of average lengths of cutting edges of knives in operation	$C_p$	Material constant
$k_A$	Specific surface digging resistance per cross-sectional area of segments	$m_p$	Material constant
$A_{sr}$	Average cross-sectional areas of segments	$\Delta K$	Fatigue load
$\varphi$	Angle of digging	$Y$	geometric factor
$F_k$	Overall digging resistance (spatial load)	$a$	Pre-crack depth
$F_t$	Tangential component of spatial load	$b$	Specimen width
$F_n$	Normal component of spatial load	$W$	Specimen height
$F_b$	Lateral component of spatial load	$K_{IC}$	Critical value of stress intensity
$N$	Nominal digging power	$a_0$	Length of initial crack that existed at tested specimens
$N_k$	Power required for digging	$a_{cr}$	Calculated critical length of edge crack
$N_h$	Dug material	$T_y$	Excavator's average number of operating hours per year
$F(\varphi)$	Digging resistance of a bucket at specific angle	$N_y$	Overall number of stress variation cycles
$T(\varphi)$	Rotational moment of the bucket-wheel shaft	$n_{bw}$	Number of revolutions of the bucket-wheel
$XK$	System rigidity matrix	$n_B$	Number of buckets
$M$	Mass matrix		

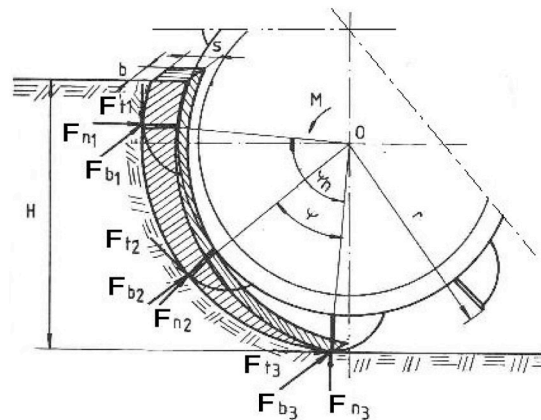


Fig. 2. Digging resistances for the bucket-wheel excavator SchRs 650/5 × 24.

product of the specific surface digging resistance per cross-sectional area of segments  $k_A$ , [kN/m<sup>2</sup>] and the sum of average cross-sectional areas of segments  $A_{sr}$  [m<sup>2</sup>] depending on the number of buckets on the bucket-wheel ( $z$ ) and the angle of digging  $\varphi$  [m<sup>2</sup>].

$$F_t = \left\{ k_L \cdot L_{sr}; L_{sr} = \frac{z}{2\pi} \cdot \int_0^{\varphi\alpha} L(\varphi) d\varphi, k_L \cdot A_{sr}; A_{sr} = \frac{z}{2\pi} \cdot \int_0^{\varphi\alpha} L(\varphi) d\varphi \right\} \quad (1)$$

Overall digging resistance  $F_k$  represents the spatial load, which consists of 3 components: tangential component  $F_t$ , normal component  $F_n$  (due to the rotation of the bucket-wheel), and lateral component  $F_b$  (due to the circular motion of the superstructure

with the cutting wheel and the boom:

$$F_k = \sqrt{F_t^2 + F_n^2 + F_b^2}; F_n = \psi_n \cdot F_t; F_b = \psi_b \cdot F_t \tag{2}$$

where:  $\psi_n$  and  $\psi_b$  - experimental proportionality coefficients, which depend on the operating environment.

Nominal digging power  $N$  [kW], which depends on the efficiency of electric motors  $\eta$ , can be defined as the sum of the power required for digging  $N_k$  and power required for lifting and loading of the dug material  $N_h$ :

$$N = \frac{1}{\eta} \cdot (N_k + N_h) \tag{3}$$

Based on the characteristics of the digging resistance of a bucket  $F_{i(\varphi)}$ , as a random function of the angle of digging, it is possible to move on to static characteristics of the cumulative bucket-wheel shaft load  $F(\varphi)$  and rotational moment of the bucket-wheel shaft  $T(\varphi)$ . Magnitudes  $F(\varphi)$  and  $T(\varphi)$  are valid for the dimensioning of drive systems. Their accurate values are being obtained through measurements on a large number of buckets and bucket-wheel excavators in various digging environments.

### 2.1.2. Measurement of the digging resistance

Measurement of the digging resistance is being performed directly at the bucket-wheel excavator and in the laboratory (measurement through the use of the pendulum, wedge, penetrometer, triaxial apparatus, ultrasound device).

For the measurement of digging resistances Wattmeter method is most commonly being used. This method is based on the measurement of the actual power on the transmission gearbox of the bucket-wheel drive. On the basis of acquired data regarding the current intensity and voltage measured through the use of the wattmeter, the actual power is being calculated and recorded as time dependent power variation. Electric energy consumption is a consequence of overcoming all resistances during the digging process.

## 2.2. Deformations and operational stresses

Conditions of exploitation of a bucket-wheel excavator may vary and depend on a large number of deterministic and random parameters. In order to determine the actual stress state of certain structures and stress variation with time it is necessary to perform deformation variation measurements and calculate the stresses.

### 2.2.1. Deformation measurement

On the basis of tensometric measurements of deformations in various conditions of exploitation performed through the use of strain gauges, the stresses at which plastic deformations and initial cracks occur on the shaft of the bucket-wheel drive have been calculated. Measurements have been performed through the use of four XY-120-HBM strain gauges, adequate for the measurement of deformations caused by the moment of rotation. Electric signal has been brought from the drive shaft to the measurement equipment for the registration and processing of signals through the use of special sliding copper rings, positioned in the near proximity of the bucket-wheel, as well as through the use of graphite brushes positioned on stationary bearers (Fig. 3).

During the test the 4-channel magnetic recorder HP-3964-A, adjusted to record and reproduce in dynamic operating conditions was used. Visual monitoring of deformations during the test, in order to prevent overstepping of prescribed values, has been performed through the use of the single channel oscilloscope. For the drawing of records suitable for the analysis graphic recorders were used, which can amplify the signal within the range from 1 [μV] to 500 [V] and stretch the signal within the range from 1 [cm/h] to 60 [cm/min].

### 2.3. Natural and forced oscillations of the excavator

The connection of the upper rotating part and the smaller part of the bucket-wheel excavator is, taking into account the bucket-wheel boom, discharge boom and the counterweight, insufficiently strong to provide structural stability during operation. Bucket-wheel excavators are thus being brought into oscillatory state very easily, in stationary as well in non-stationary operation regimes,

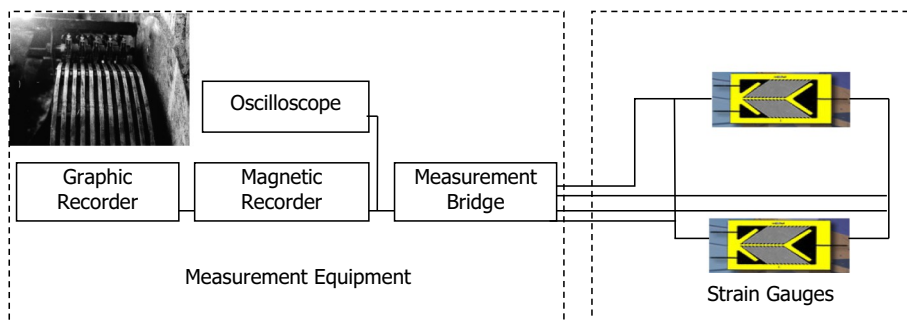


Fig. 3. Overview of the structure of signal processing measurement equipment with copper rings and graphite brushes.

and the oscillations of support structures induced in such a way cause the occurrence of dynamic loads in structural elements. These oscillations can be very complex and of a wide frequency range.

2.3.1. Theoretical analysis

Oscillations of the support structures of the bucket-wheel excavator are being characterized by translational and/or rotational movement of cross-section points, or by their displacement from the neutral position, which is time dependant  $Y = y(t)$ .

On the basis of technical documentation and dimensions of structural elements, the calculation of stick forces and displacement of spatial lattice knots, as well as the calculation of masses and rigidness coefficients for individual sticks are being performed. Nevertheless, natural vertical oscillations of the boom have been calculated through the use of the „Finite-storrelemente” method [14], on the spatial lattice model, Fig. 4.

During the calculation of frequencies of natural oscillations, it has been assumed that masses of rigid elements are concentrated in nodes and that elastic elements are positioned in directions convergent to directions of sticks in the lattice model (Fig. 4). On the basis of the displacement of the mass of every stick and every node the overall mass of the lattice has been determined. Impact load can have big effect on dynamic buckling of lattice shown by Liu et al. [15].

Frequencies of natural vertical oscillations have been obtained from the following equation:

$$\det(XK - f^1M) = 0 \tag{4}$$

where: XK - system rigidness matrix and M - mass matrix.

Such obtained approximate values of frequencies of natural oscillations for the approximate model of the bucket-wheel boom are  $f_{\min} = 4.58$  [Hz] and  $f_{\max} = 195.0$  [Hz].

3. Results

3.1. Results of measurement of digging resistances

In these researches measurements on the bucket-wheel excavator have been performed under the operational load in various digging environments. Fig. 5 presents the record of the current intensity variation with respect to the size of the segment, while Fig. 6 presents the record on which marked points represent:

- Point 1 - current intensity in the moment of motor start-up,
- Point 2 - current intensity during the idle operation of the bucket-wheel,
- Point 3 - current intensity during digging,
- Point 4 - highest recorded value of current intensity in the diagram.

Taking into account the data regarding the actual power of the bucket-wheel drive system  $N$  [kW] and adequate hourly production  $Q_e$  [m<sup>3</sup>/h], recorded during the excavator operation in various digging environments, the statistical analysis has been performed through the use of the method of least squares, and linear correlations for the regressive function  $N = N(Q_e)$  were established, as shown in Fig. 7:

– loose overburden  $N(Q_e) = 0.0837Q_e + 229.6$  (5)

– compact grey clay  $N(Q_e) = 0.1666Q_e + 366.6$  (6)

Through the analysis of histograms of the empirical distribution, cumulative frequency functions and statistical characteristics it has been established that normal law of distribution is suitable for the mathematical depiction of random values of the specific digging resistance per knife length ( $k_t$ ) (Fig. 8).

In Table 1 values of parameters of the normal law of distribution of the specific digging resistance per knife length and results of the acceptance test of the law based on the coefficient of variation are presented.

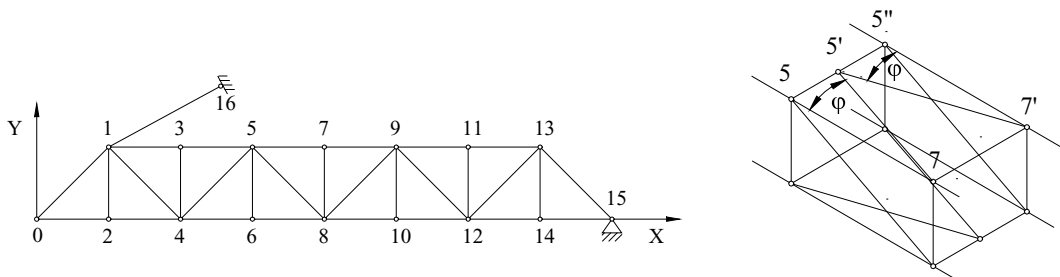


Fig. 4. Calculation model of the bucket-wheel boom for vertical oscillations.

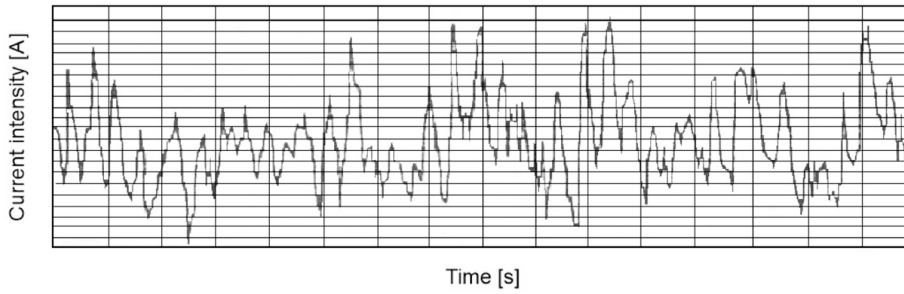


Fig. 5. Display of the partial record of current intensity variation with respect to the size of the section.

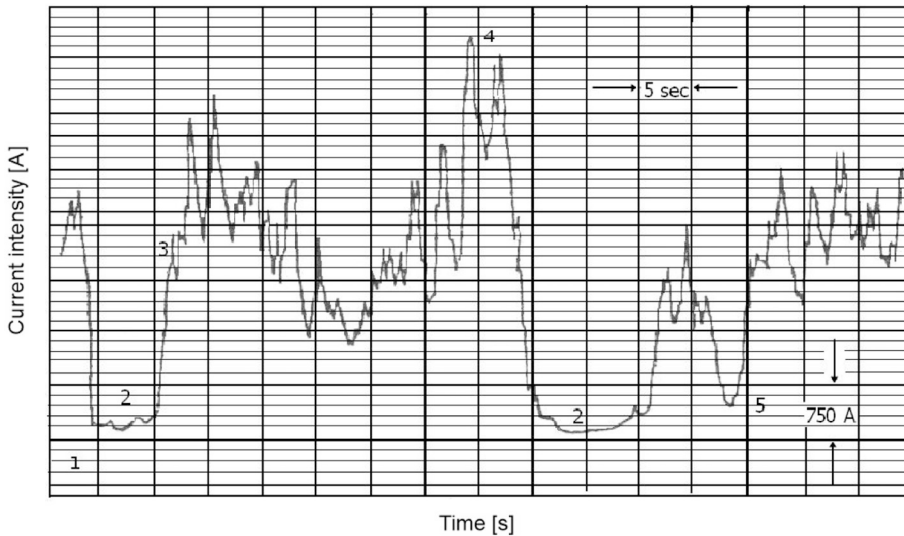


Fig. 6. Display of current intensity variation record with characteristic load points.

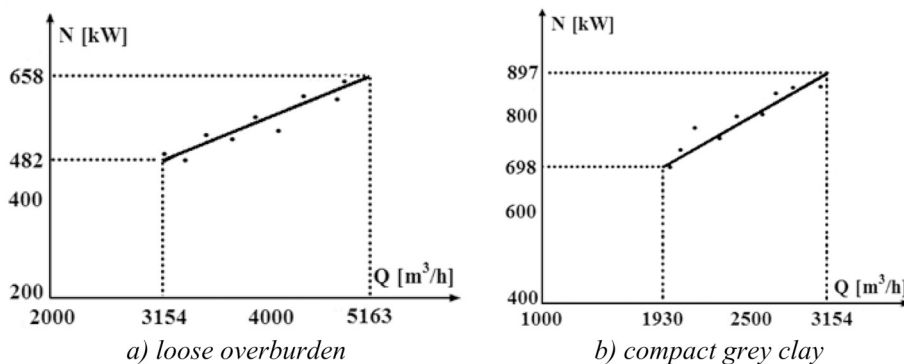


Fig. 7. Power variation with respect to hourly production.

### 3.2. Results of deformation measurements

Values of stresses at the drive shaft of the bucket-wheel, according to deformations recorded for every monitored load regime, are presented in Table 2. A short record which refers to bucket-wheel start-up and its operation under average load conditions and stopping is shown in Fig. 9.

#### 3.2.1. The assessment of gearbox lifetime on the basis of measured deformations

Measurement results, presented by normal deformation  $\epsilon$ , were converted into tangential stresses  $\tau$  through the introduction of the modulus of elasticity  $E$  and Poisson's ratio  $\nu$  which, along with the polar moment of inertia of the bucket-wheel drive shaft cross-

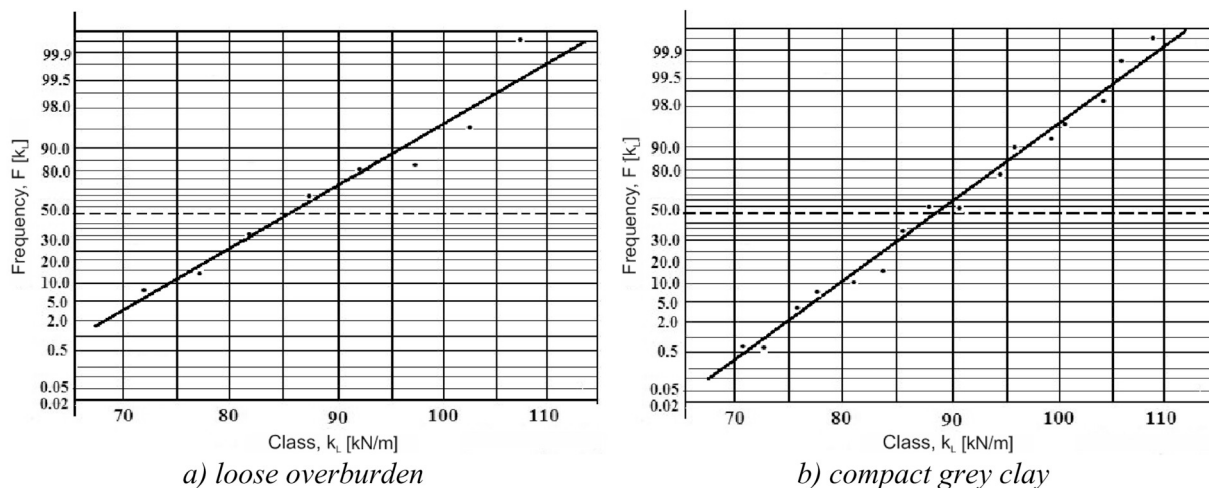


Fig. 8. Graphic determination of parameters of the normal law of distribution.

Table 1

Parameters of the normal law of distribution of the specific digging resistance per knife length.

	Normal distribution			
	Mean value	Standard deviation	Variation	Test for extreme values
	$k_L^*$ [kN/m]	$\sigma$ [MPa]	$V = \sigma/k_L$	$k_L^* \cdot 3\sigma$
Maximum loads	86.3	23.2	0.27	Satisfiable
All measurements	68.2	19.1	0.28	Satisfiable

$$f_i = \frac{1}{\sigma\sqrt{2\pi}} e^{-\frac{1}{2}\left(\frac{k_L k_L^*}{\sigma}\right)^2}$$

Table 2

Stresses calculated on the basis of measured deformations at the drive shaft of the bucket-wheel.

No.	Tested operation regimes of the bucket-wheel excavator	Calculated stresses $\tau$ [MPa]
1	Idle operation	25
2	Average load during the digging of loose overburden	46
3	Highest load during the digging of loose overburden	69
4	Average load during the digging of compact grey clay	86
5	Highest load during the digging of compact grey clay	98

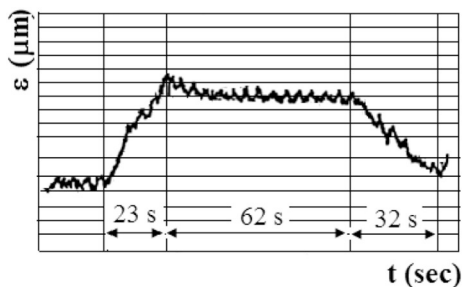


Fig. 9. Display of the short deformation - time record.

section  $W_p$ , define moments of rotation (torsional moments)  $T_i$  on the outgoing bucket-wheel drive shaft, which could be used for the assessment of gearbox lifetime.

$$\tau = \frac{\varepsilon \cdot E}{1 + \nu}; \quad T = W_0 \cdot \tau \tag{7}$$

The application factor  $K_A$  for the gear with the largest number of revolutions has been obtained through the use of the load - capacity comparison method via maximization of the ratio of their indicators. This factor takes into account the influence of the external load variation on the gearbox lifetime with certain approximations regarding the loading regimes during various phases of exploitation and was determined for standard numerals which are defined with respect to the gear tooth root, because theoretical analyses performed according to [14] showed that the gear tooth root safety is smaller than gear tooth flank safety. For applications in structures exploited in dynamical conditions (subjected to cyclic torque and torsional vibrations) such as marine gears, excavators etc., the application factor can be defined as the ratio between the equivalent cyclic torque and the nominal torque. The application factor  $K_A$  was calculated according to Eq. (8) [16]:

$$K_A = \frac{T_{eq}}{T_n}, \tag{8}$$

where:  $T_{eq}$  is equivalent torque and  $T_n$  - the nominal torque.

For calculation values that were used are as follows:  $T_{eq} = 98 \text{ MPa}$  (Table 2) – the biggest stress and for  $T_n = 60 \text{ MPa}$  (producer's recommendation was 60–65 [9]). Based on that, calculated application factor  $K_A$  is 1.6. Value of 60 MPa was adopted in order to determine application factor for the worse working conditions.

### 3.3. Results of oscillation measurements

The measurements of vertical and horizontal displacements of speeds and accelerations under various load regimes and on hard soil sites when impact loads occur were performed in order to complete the analysis of natural and forced oscillations of the bucket-wheel boom structure. Measurements have been performed at centers of support vertical columns and at centers of main girders, in the area of the upper strip of the bucket-wheel boom, by the vibration method performed through the use of sound and vibration analyzers manufactured by “General Radio Company”.

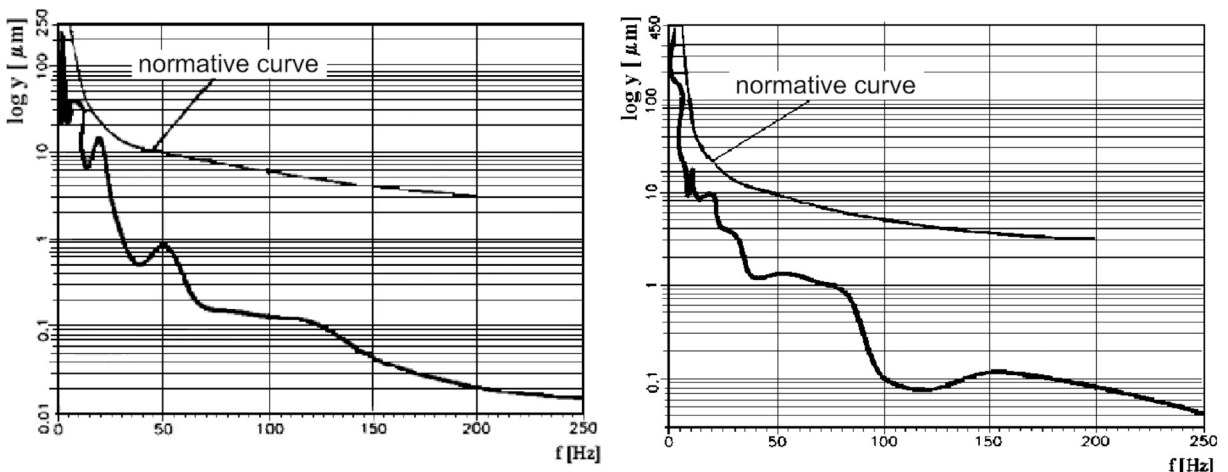
Through the analysis of oscillations during transport and operational movements of the excavator while not being engaged in the digging process it has been established that values of basic frequencies of natural oscillations are:

- vertical oscillations 1.0–3.2 [Hz],
- transverse oscillations 0.5–0.7 [Hz],
- longitudinal oscillations 0.4–0.5 [Hz].

Also, it has been determined that the value of the logarithmic decrement of attenuation is  $p = 0.5$ , which is a relatively small power attenuation and indicates the possibility of the occurrence of resonance.

The largest vertical oscillations during the operation of the excavator were recorded at main girders of the bucket-wheel boom in the range of frequency analysis from 2.5 to 5 [Hz]. It has therefore been confirmed that the threat of oscillations is present in the low-frequency area.

Theoretical analyses, which took into account theoretical indicators, were performed for harmonic oscillations in the frequency range from 2.5 to 250 [Hz] with the step size of 1/3 octave (1/3 octave analysis). Frequency spectra of vertical oscillations with respect to the normative curve, for measurement locations where highest vertical oscillations were recorded, are presented in Fig. 10. Oscillations in the frequency analysis range from 25 to 250 [Hz], which could be threatening if dislocation input is high, could be



Measurement location at the opposite side of the bucket-wheel drive

Measurement location at the bucket-wheel drive

Fig. 10. Frequency spectrum of vertical oscillations at the support structure of the bucket-wheel boom.

neglected on the basis of these tests.

Analyses of natural and forced oscillations show that the threat of the occurrence of resonance is biggest for the bucket-wheel boom structure in the low-frequency area.

Here should be mentioned that on these results design of the buckets can also have influence [28].

In the current part of the paper it was shown analysis of the oscillations and dynamic loads which occur at working parts of the excavators, while the second part of the paper is deal with integrity assessment and determination of residual fatigue life of welded joints at the boom of the bucket wheel excavator as one of the most loaded parts at the structure.

#### 4. Integrity assessment and determination of residual fatigue life of vital welded structure at bucket-wheel boom

Before integrity assessment and determination of residual life of structure elements, the most critical places at structure need to be determined. The most critical places at structure are assumed to be welded joints especially joints of girders and carrying structure as T joint (Fig. 11). That presumption is also confirmed in [19–33] but in order to confirm given presumption deformation measuring has to be conducted. Fatigue is one of the most common cause of failure of the structure [1–3,17,18,25–29]. Especially in case of welded girders [37] and stiffeners [38].

##### 4.1. Deformations and operating stresses at vital welded structures of the bucket-wheel boom

By studying the behaviour of parent material and welded joints of vital structures subjected to variable loading it was determined that nodes are critical locations, because 80% of fatigue cracks occur there (Fig. 11) [34].

Measuring tapes were applied in order to determine deformations and calculate the stresses at the elements of the vital welded structures of the boom in the bucket-wheel area, made of steels

St 37.2 and St 52.3 in accordance with standard DIN 17100, or to put it differently made of steels S235J2G3 and S355J2G3, in accordance with standard EN 10025–2 [19]. The objective of the stress condition check is to determine whether there is a possibility of occurrence of plastic deformations or initial cracks due to fatigue. Properties of structural non-alloyed steels S235J2G3 and S355J2G3 of which metal sheets and profiles were made are presented in Tables 3 and 4 and it was taken from appropriate standard [20].

##### 4.1.1. Deformation measurement

Measurements of strains at elements of the vital welded structures in the bucket-wheel area have been performed through the use of 12 measurement tapes HBM 6/350 × XY31. Structure of measurement equipment for registration and processing of electric signals (HBM Spider 8 – measurement device with 8 channels) is shown in Fig. 12.

In Fig. 13 locations where gauges for measurement of strains at the elements of vital welded structures of the boom in the bucket-wheel area subjected to various conditions of coal mining (dynamic loading) are shown.

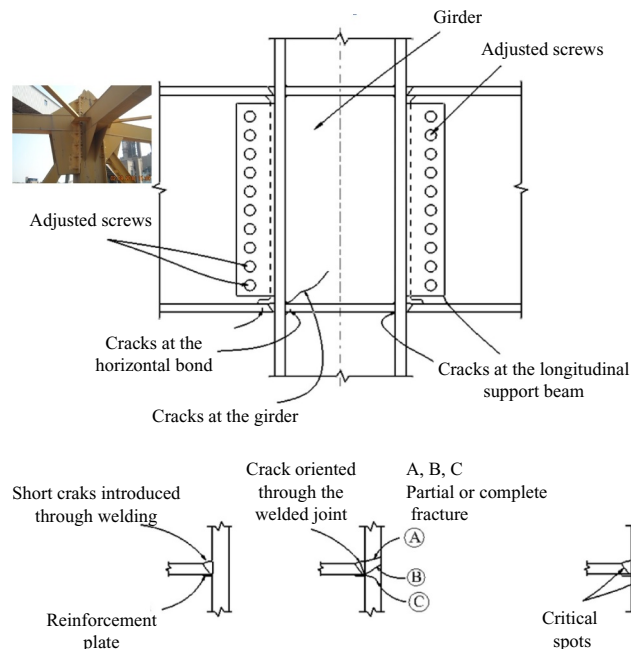


Fig. 11. Appearance of a node at the welded structure and locations at which fatigue cracks mainly occur.

**Table 3**  
Chemical composition, mass percentage [20].

Steel	C [%]	Si [%]	Mn [%]	P [%]	S [%]	Cu [%]	CEV [%]
S235J2G3	≤ 0.17	≤ 0.55	≤ 1.40	≤ 0.045	≤ 0.045	≤ 0.40	≤ 0.38
S355J2G3	≤ 0.23	≤ 0.60	≤ 1.70	≤ 0.045	≤ 0.045	≤ 0.45	≤ 0.47

**Table 4**  
Mechanical properties [20].

Steel	Yield strength $R_{eH}$ [MPa]	Tensile strength $R_m$ [MPa]	Elongation $A_5$ [%]
S235J2G3	235	360–510	24
S355J2G3	355	470–630	22

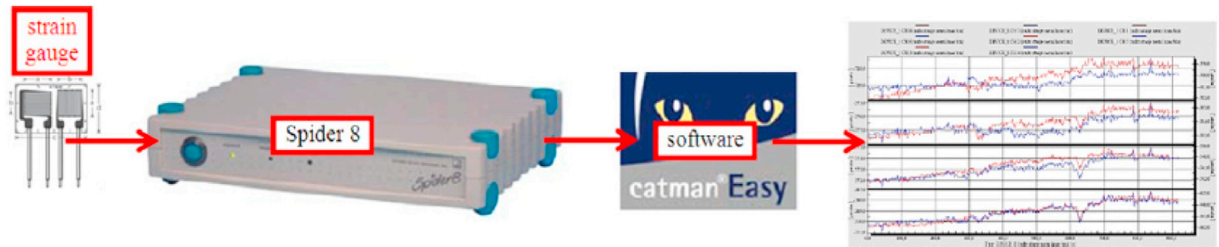


**Fig. 12.** Appearance of the measurement equipment for registration and processing of electric signals (HBM Spider 8 – measurement device with 8 channels).



**Fig. 13.** Welded structure of the bucket-wheel boom and spots where strain gauges were located.

Locations where deformations were measured at vertical girders (M1–M4), horizontal girders (M5–M8) and diagonals (M9–M12) were selected on the basis of design and technical documentation, in order to enable insight in stress condition at characteristic locations of the welded structure of the boom in the area of the bucket-wheel. Gauges M3 and M4 are not visible at Fig. 13 since their position is symmetric to gauges M1 and M2, but on the opposite side of the boom.

#### 4.2. Stresses at the elements of the vital welded structure of the boom in the area of the bucket-wheel

On the basis of calculated stresses at the elements of the vital welded structure of the boom in the area of the bucket-wheel (Fig. 4), presented in Tables 5 and 6, it can be concluded that stresses are in linear elastic area and that they are 50% lower than yield stress for steels S235J2G3 and S355J2G3. Highest values of stress were determined for diagonals.

**Table 5**

Calculated stresses at vertical and horizontal girders of the boom structure in the bucket-wheel area close to nodes of the structure elements,  $\sigma_1$  [MPa].

Operational mode of the bucket-wheel excavator	Measurement locations							
	M1	M2	M3	M4	M5	M6	M7	M8
Average load during the digging of loose overburden	54.8	58.2	54.2	46.4	45.7	47.1	45.3	42.8
Full cut load during the digging of loose overburden	57.3	62.8	57.3	50.6	48.6	50.9	48.1	44.3
Average load during the digging of compact grey clay	67.6	70.1	59.9	53.2	55.1	57.4	54.2	48.8
Full cut load during the digging of compact grey clay	73.9	73.9	67.3	58.6	59.3	62.1	60.7	54.3

**Table 6**

Calculated stresses at diagonals of the boom structure in the bucket-wheel area close to nodes of the structure elements,  $\sigma_1$  [MPa].

Operational mode of the bucket-wheel excavator	Measurement locations			
	M9	M10	M11	M12
Average load during the digging of loose overburden	65.5	59.3	60.5	54.2
Full cut load during the digging of loose overburden	97.7	63.9	67.7	57.6
Average load during the digging of compact grey clay	114.9	75.6	69.2	62.7
Full cut load during the digging of compact grey clay	145.5	108.4	102.8	93.1

Taking into account the fact that tests by which the stress condition of elements of the vital welded structure of the bucket-wheel boom was determined did not comprise boundary loads which occur during the digging of petrified rock masses, when due to impact loads bucket-wheel halts, the limit of useful load can not be determined.

4.3. Determination of fracture mechanics parameters

Behaviour of material with a single crack subjected to variable loads is defined by parameters which are being obtained by examination of the growth of the fatigue crack, and those are fatigue crack growth rate ( $da/dN$ ) and minimum critical stress intensity factor at which there is no crack growth (fatigue threshold). Area of stable growth of the fatigue crack is formulated by Paris - Erdogan equation (Eq. (9)) [22,24].

$$\frac{da}{dN} = C_p \cdot (\Delta K)^{m_p} \tag{9}$$

For the service life assessment and integrity evaluation of the vital welded structure of the boom in the area of the bucket-wheel, determination of parameters of fracture mechanics was carried out at 4 specimens extracted from samples of sheet metal made of steel S355J2G3 (Fig. 14) taken from the area of measurement location 9 (Fig. 13). On the basis of the crack growth rate  $da/dN$  lengths of critical cracks  $a_c$  were calculated [22]. Pre-crack is located in heat affected zone (HAZ) as the most critical zone of the welded joint [35].

Geometric member  $Y(a_0/W)$  for specimens subjected to testing was calculated through the use of the following equation [7,22]:

$$Y(a_0/W) = \frac{3 \cdot (a_0/W)^{1/2} \cdot [1.99 - (a_0/W) \cdot (1 - a_0/W) \cdot (2.15 - 3.93 \cdot (a_0/W) + 2.7 \cdot (a_0/W)^2)]}{2 \cdot (1 + 2a_0/W) \cdot (1 - a_0/W)^{3/2}} \tag{10}$$

Device for determination of the growth rate of fatigue cracks by alternate bending “Cracktronic” is presented in Fig. 15.

One of dependency curves  $a - N$  (crack length dependent on load cycles), presented in Fig. 16, shows that growth of initial crack from 2 mm to 3.58 mm starts slowly and has a rapid progress afterwards.

Values of measured and calculated parameters of fracture mechanics for the highest possible value of the stress range  $\Delta\sigma = 145.5$  MPa on the basis of the mean value of fatigue crack growth rate for 4 specimens are as follows:

$Y(a/W) = 2.32$  – parameter which depends on specimen geometry and crack shape,

$\Delta\sigma = 145.5$  MPa – highest possible value of the stress range,

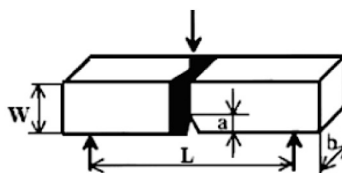


Fig. 14. Appearance of the specimen tested in order to determine the growth rate of the fatigue crack.

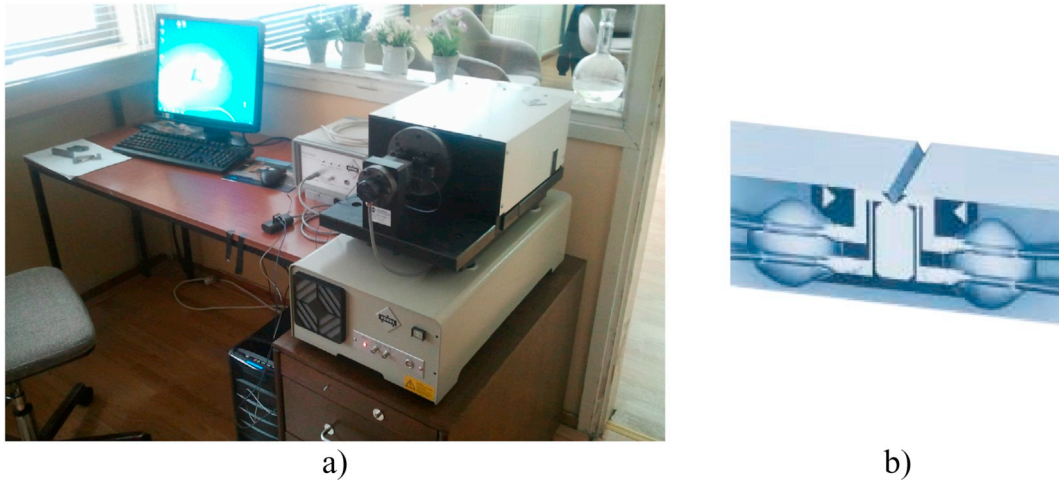


Fig. 15. Appearance of the device (a) and a specimen with strain gauge for determination of the growth rate of fatigue cracks (b) [24]

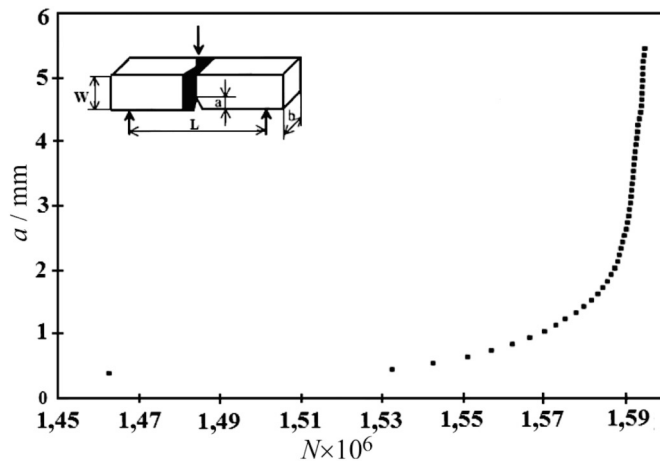


Fig. 16. An experimentally obtained  $a - N$  curve.

$C_p = 1.58 \cdot 10^{-14}$  ( $m_p$ ,cycle)/(MPa  $\cdot \sqrt{m}$ ) <sup>$m_p$</sup>  - Paris-Erdogan equation constant,  
 $m_p = 3.55$  - Paris-Erdogan equation constant,  
 $K_{IC} = 126.5$  MPa  $\cdot \sqrt{m}$  - critical value of stress intensity,  
 $a_0 = 2$  mm - length of initial crack that existed at tested specimens,  
 $a_{cr} = 44.65$  mm - critical length of edge crack calculated through the use of Eq. (11) [8,22]:

$$a_{cr} = \frac{1}{\pi} \cdot \left( \frac{K_{IC}}{\Delta\sigma \cdot Y} \right)^2 \rightarrow a_{cr} = \frac{1}{3.14} \cdot \left( \frac{4000}{145.5 \cdot 2.32} \right)^2 = 44.65 \text{ mm} = 0.04465 \text{ m} \tag{11}$$

For the above mentioned welded structure the remaining number of load cycles for the bucket-wheel excavator is being obtained from Eq. (9):

$$\begin{aligned} \frac{da}{dN} &= C_p \cdot (\Delta K)^{m_p} \rightarrow N a_0 - N a_{ck} = N = \frac{1}{\left(\frac{m_p-2}{2}\right) \cdot C_p \cdot f^{m_p} \cdot \pi^{\frac{m_p}{2}} \cdot \Delta\sigma^{m_p}} \left[ \frac{1}{a_0^{\frac{m_p-2}{2}}} - \frac{1}{a_{cr}^{\frac{m_p-2}{2}}} \right] = \\ &= \frac{1 \cdot 10^{14}}{\left(\frac{3.55-2}{2}\right) \cdot 1.55 \cdot 2.32^{3.55} \cdot 3.14^{\frac{3.55}{2}} \cdot 145.5^{3.55}} \left[ \frac{1}{0.002^{\frac{3.55-2}{2}}} - \frac{1}{0.04465^{\frac{3.55-2}{2}}} \right] = 1.182 \cdot 10^7 \text{ cycles} \end{aligned} \tag{12}$$

For the average number of operating hours per year  $T_y = 4250$  h, the overall number of stress variation cycles is:

$$N_y = 60 \cdot T_y \cdot n_{BW} \cdot n_B = 60 \cdot 4250 \cdot 4.86 \cdot 21 = 2.6 \cdot 10^6 \text{ cycles/year} \tag{13}$$

where:  $T_y = 4250$  h – average number of operating hours of the bucket-wheel excavator per year,  $n_{bw} = 4.86$  rpm – number of revolutions of the bucket-wheel,  $n_B = 21$  – number of buckets.

Based on determined parameters of fracture mechanics, the service life of the carrying welded structure in the area of the bucket-wheel at maximum expected load after the repair of the existing damage, in case of initiation of a new edge crack in the longitudinal direction of sheet metal is being obtained from Eq. (6) as:

$$n = \frac{N}{N_U} = \frac{1.182 \cdot 10^7}{2.6 \cdot 10^6} = 4.55 \text{ years} \quad (14)$$

## 5. Conclusion

Fatigue failures often occur in highly-stressed structural components of machines during exploitation. In the present case, failure analysis and service life determination was done for complex structure of bucket-wheel excavator SchRs 650/5 × 24 Krupp. Based on presented results and analysis, the following conclusions can be drawn:

- Specific digging resistances per knife length ( $k_L$ ) at highest recorded loads are 20% higher than the average value for overall measurements in various digging environments, but at the same time smaller than the designed value. Determined linear correlations for the regressive function of actual power of the bucket-wheel drive system and adequate hourly production  $N = N(Q_e)$ , show that the bucket-wheel excavator during operation, when compact grey clay is concerned, cannot reach the designed (theoretical) capacity  $Q_t = 4212 \text{ [m}^3/\text{h]}$ .
- Application factor  $K_A$  was used to predict the load capacity of gear drives during cyclic loading in exploitation. In that order, for every monitored load regime the deformations were measured and the level of stresses were determined. For every analyzed case the stress level was within predicted ranges. Also, determined value of the application factor  $K_A = 1.6$  is smaller than the one prescribed in appropriate standards ISO 6336-1:2006 [36] and DIN 3990 for the gearbox of the bucket-wheel drive, according to which  $K_A = 1.75\text{--}2.0$ . This case is more desirable for the gearbox from the aspect of the reliability, since there is a possibility to apply greater loads.
- Frequency analyses of oscillations for various excavator operations show that all oscillations are within the allowable range, but with sudden variations. In case of very frequent sudden variations should be careful since there is a possibility of the occurrence of resonance due to matching of natural oscillations of the structure and oscillations caused by the action of the periodic load and therefore of the occurrence of quick damaging of critical cross-sections.
- From the aspect of structural integrity, values of measured and calculated parameters of fracture mechanics for the highest possible value of the stress range were  $\Delta\sigma = 145.5 \text{ MPa}$ , what is less than yield strength of the weakest element in structure.
- For given conditions critical length of edge crack was calculated as  $a_{cr} = 44.65 \text{ mm}$  and based on that and the average number of operating hours per year, the overall number of stress variation cycles was determined, what was necessary to determine excavator's service life of 4.55 years in case of initiation of a new edge crack in the longitudinal direction of sheet metal.

Realized researches and results presented in this paper offer great possibilities to designers of bucket-wheel excavators to carry out behaviour analyses for vital welded structure of the boom in the area of the bucket-wheel. Here should be emphasize the fact that tests by which the stress condition of elements of the vital welded structure of the bucket-wheel boom was determined did not comprise boundary loads which occur during the digging of petrified rock masses, when due to impact loads bucket-wheel halts, the limit of useful load can not be determined.

## Acknowledgment

Authors wish to thank the Ministry of Education, Science and Technological Development of Republic of Serbia for financial support through the projects TR 35006 and TR 35024.

## References

- [1] S. Bošnjak, M. Arsić, N. Zrnić, M. Rakin, M. Pantelić, Bucket wheel excavator: integrity assessment of the bucket wheel boom tie-rod welded joint, *Eng. Fail. Anal.* 18 (2011) 212–222, <https://doi.org/10.1016/j.engfailanal.2010.09.001>.
- [2] M. Arsić, S. Bošnjak, N. Zrnić, A. Sedmak, N. Gnjatović, Bucket wheel failure caused by residual stresses in welded joints, *Eng. Fail. Anal.* 18 (2011) 700–712, <https://doi.org/10.1016/j.engfailanal.2010.11.009>.
- [3] S. Bošnjak, M. Arsić, N. Gnjatović, I. Milenović, D. Arsić, Failure of the bucket wheel excavator buckets, *Eng. Fail. Anal.* 84 (2018) 247–261, <https://doi.org/10.1016/j.engfailanal.2017.11.017>.
- [4] S. Bošnjak, M. Arsić, S. Savićević, G. Milojević, D. Arsić, Fracture analysis of the pulley of a bucket wheel boom hoist system, *Ekspl. Niez. Maint. Reliab.* 18 (2) (2016) 155–163, <https://doi.org/10.17531/ein.2016.2.1>.
- [5] Dj. Djurdjevic, T. Maneski, V. Milosevic-Mitic, N. Andjelic, D. Ignjatovic, Failure investigation and reparation of a crack on the boom of the bucket wheel excavator ERS 1250 Gacko, *Eng. Fail. Anal.* 92 (2018) 301–316, <https://doi.org/10.1016/j.engfailanal.2018.05.015>.
- [6] Ž. Lazarević, I. Arandelović, S. Kirin, An analysis of random mechanical failures of bucket wheel excavator, *Struct. Integr. Life* 15 (3) (2015) 143–146.
- [7] M. Arsić, S. Bošnjak, Z. Odanović, M. Dunjic, A. Simonovic, Analysis of the spreader track wheels premature damages, *Eng. Fail. Anal.* 20 (2012) 118–136, <https://doi.org/10.1016/j.engfailanal.2011.11.005>.
- [8] M. Arsić, S. Bošnjak, N. Gnjatović, S.A. Sedmak, D. Arsić, Z. Savić, Determination of residual fatigue life of welded structures at bucket-wheel excavators through the use of fracture mechanics, *Proc. Struct. Integr.* 13 (2018) 79–84, <https://doi.org/10.1016/j.prostr.2018.12.014>.
- [9] Technical Documentation of Excavator SchRs 650/5 × 24, Thyssen Krupp Company, Germany.
- [10] S.M. Bošnjak, D.C.D. Oguamanam, N.Đ. Zrnić, The influence of constructive parameters on response of bucket wheel excavator superstructure in the out-of-resonance region, *Arch. Civ. Mech. Eng.* 15 (4) (2015) 977–985, <https://doi.org/10.1016/j.acme.2015.03.009>.

- [11] D. Pietrusiak, P. Moczko, T. Smolnicki, E. Rusiński, Identification of low cycle dynamic loads acting on heavy machinery, *Procedia Eng.* 199 (2017) 254–259, <https://doi.org/10.1016/j.proeng.2017.09.017>.
- [12] I. Cires, V.M. Nani, Stability control for a huge excavator for surface excavation, *Appl. Math. Model.* 40 (2016) 388–397, <https://doi.org/10.1016/j.apm.2015.04.056>.
- [13] S. Bošnjak, N. Gnjatović, I. Milenović, From 'a priori' to 'a posteriori' static stability of the slewing superstructure of a bucket wheel excavator, *Ekspl. Niez. Maint. Reliab.* 20 (2) (2018) 190–206, <https://doi.org/10.17531/ein.2018.2.04>.
- [14] M. Arsić, V. Aleksić, Z. Aleksić, Experimental Analysis upon Rotating Wheel Operating Loading of the Bucket Wheel SchRs 650/5×24, 6th European Coal Conference COAL 05, Belgrade, (2005), pp. 325–331.
- [15] M.S. Liu, J.Y. Li, Z.X. Tian, C.W. Zhu, J.S. Ju, Effect of impact load on dynamic buckling of steel lattice arch, *Strength Mater.* 49 (1) (2017) 45–54, <https://doi.org/10.1007/s11223-017-9840-1>.
- [16] F. Curà, Method for calculating the application factor  $K_A$  in gears subjected to variable working conditions, *Procedia Eng.* 101 (2015) 109–116, <https://doi.org/10.1016/j.proeng.2015.02.015> (ISSN: 1877-7058).
- [17] N. Zrnić, S. Bošnjak, V. Gašić, M. Arsić, Z. Petković, Failure analysis of the tower crane counterjib, *Procedia Eng.* 10 (2011) 2238–2243, <https://doi.org/10.1016/j.proeng.2011.04.370>.
- [18] H. Guo, J. Wan, Y. Liu, J. Hao, Experimental study on fatigue performance of high strength steel welded joints, *Thin-Walled Struct.* 131 (2018) 45–54, <https://doi.org/10.1016/j.tws.2018.06.023>.
- [19] C. Cui, Q. Zhang, Y. Bao, J. Kang, Y. Bu, Fatigue performance and evaluation of welded joints in steel truss bridges, *J. Constr. Steel Res.* 148 (2018) 450–456, <https://doi.org/10.1016/j.jcsr.2018.06.014>.
- [20] EN 10025-2:2004, Hot Rolled Products of Structural Steels - Part 2: Technical Delivery Conditions for Non-alloy Structural Steels, European Committee for Standardization, 2005.
- [21] V. Lazić, D. Arsić, I. Ilić, S. Aleksandrović, R. Nikolić, M. Djordjević, B. Hadzima, Qualification of the welding technology of the structural steel S355J2G3, *IOF Conf. Ser. Mat. Sci. Eng.* 419 (2018) 1–12, <https://doi.org/10.1088/1757-899X/419/1/012019>.
- [22] P.W. Hertzberg, R. Vinci, J.L. Hertzberg, *Deformation and Fracture Mechanics of Engineering Materials*, fifth ed., John Wiley & Sons Inc, New York, 2012.
- [23] ASTM E 647-15e1, Standard Test Method for Measurement of Fatigue Crack Growth Rates, ASTM International, 2015.
- [24] I. Čamagić, N. Vasić, Z. Vasić, Z. Burzić, A. Sedmak, Compatibility of fracture mechanics parameters and fatigue crack growth parameters in welded joint behaviour evaluation, *Tehn. vjes. Tech. Gazz.* 20 (2) (2013) 205–211.
- [25] E. Rusiński, P. Harnatkiewicz, M. Kowalczyk, P. Moczko, Examination of the causes of a bucket wheel fracture in a bucket wheel excavator, *Eng. Fail. Anal.* 17 (2010) 1300–1312, <https://doi.org/10.1016/j.engfailanal.2010.03.004>.
- [26] D. Danicic, S. Sedmak, D. Ignjatovic, S. Mitrovic, Bucket wheel excavator damage by fatigue fracture – case study, *Proc. Math. Sci.* 3 (2014) 1723–1728, <https://doi.org/10.1016/j.mspro.2014.06.278>.
- [27] J. Czmochoowski, P. Maslak, P. Dzialak, G. Przybyłek, M. Stanco, Assessment methodology of a technical condition of the bucket chain excavator structure, *Mat. Today Proc.* 4 (2017) 5785–5790, <https://doi.org/10.1016/j.matpr.2017.06.046>.
- [28] E. Rusinski, L. Cegiel, A. Michalczuk, P. Moczko, J. Olejarz, D. Pietrusiak, Investigation and modernization of buckets of surface mining machines, *Eng. Struct.* 90 (2015) 29–37, <https://doi.org/10.1016/j.engstruct.2015.02.009>.
- [29] M. Kepka, M. Kepka Jr., Deterministic and probabilistic fatigue life calculations of a damaged welded joint in the construction of the trolleybus rear axle, *Eng. Fail. Anal.* 93 (2018) 257–267, <https://doi.org/10.1016/j.engfailanal.2018.07.015>.
- [30] F.M. José, A.F.O. Correia, A.M.P. de Jesus, Á. Cunha, E. Caetano, A.A. Fernandes, Fatigue analysis of a railway bridge based on fracture mechanics and local modelling of riveted connections, *Eng. Fail. Anal.* 94 (2018) 121–144, <https://doi.org/10.1016/j.engfailanal.2018.07.016>.
- [31] A. Sghayer, A. Grbović, A. Sedmak, M. Dinulović, E. Doncheva, B. Petrovski, Fatigue life analysis of the integral skin-stringer panel using XFEM, *Struct. Integr. Life* 17 (1) (2018) 7–10.
- [32] A. Grbović, A. Sedmak, G. Kastratović, D. Petrašinović, N. Vidanović, A. Sghayera, Effect of laser beam welded reinforcement on integral skin panel fatigue life, *Eng. Fail. Anal.* 101 (2019) 383–393, <https://doi.org/10.1016/j.engfailanal.2019.03.029>.
- [33] A. Sedmak, Computational fracture mechanics: an overview from early efforts to recent achievements, *Fatigue Fract. Eng. Mater. Struct.* 41 (2018) 2438–2474, <https://doi.org/10.1111/ffe.12912>.
- [34] S. Sedmak, R. Jovičić, A. Sedmak, M. Arandelović, B. Đorđević, Influence of multiple defects in welded joints subjected to fatigue loading according to SIST EN ISO 5817:2014, *Struct. Integr. Life* 18 (1) (2018) 77–81.
- [35] B. Younise, M. Rakin, N. Gubeljak, B. Medjo, A. Sedmak, Effect of material heterogeneity and constraint conditions on ductile fracture resistance of welded joint zones – micromechanical assessment, *Eng. Fail. Anal.* 82 (2017) 435–445, <https://doi.org/10.1016/j.engfailanal.2017.08.006>.
- [36] ISO 6336-1, Calculation of Load Capacity of Spur and Helical Gears - Part 1: Basic Principles, Introduction and General Influence Factors, International Organization for Standardization, 2006.
- [37] A.L.L.da Silva, J.A.F.O. Correia, A.M.P. de Jesus, G. Lesiuk, A.A. Fernandes, R. Calçada, F. Berto, Influence of fillet end geometry on fatigue behaviour of welded joints, *Int. J. Fatigue* 123 (2019) 196–212, <https://doi.org/10.1016/j.ijfatigue.2019.02.025>.
- [38] Ž. Božić, S. Schmauder, H. Wolf, The effect of residual stresses on fatigue crack propagation in welded stiffened panels, *Eng. Fail. Anal.* 84 (2018) 346–357.